Myelinated Nerve Fiber Response to Dynamic Uniaxial Stretch

Kathryn E. Saatman and Lawrence E. Thibault

Department of Bioengineering, University of Pennsylvania
114 Hayden Hall, Philadelphia, PA 19104, USA

ABSTRACT

The response of myelinated nerve fibers to dynamic uniaxial stretch was investigated as part of an ongoing effort to establish functional and structural failure criteria for both neural and vascular tissues. Such individual tissue failure criteria, integrated with existing knowledge from more macroscopic head injury research, could be used in the development of head injury tolerance levels for specified loading conditions.

Nerve fibers were placed in a mechanical testing apparatus capable of delivering a dynamic uniaxial displacement pulse to the fibers. Using custom-made micropipets, a single myelinated fiber was mounted in the apparatus and rapidly elongated. To monitor the pathophysiologic response of myelinated fibers, the nerves were loaded with a fluorescent dye sensitive to intracellular calcium. Thus a change in the intracellular calcium concentration could be determined by measuring the changes in emitted fluorescence.

Results show that the intracellular calcium concentration increased following rapid elongation of myelinated nerve fibers. The response of a single fiber was much like that for several fibers subjected to stretch. The increase in calcium typically occurred over 30 seconds, and under most conditions the calcium concentration returned toward the initial baseline level. However, a continued rise in calcium concentration over a two minute time period was seen following a repeated stretch to a single myelinated nerve.

INTRODUCTION

There are obviously many ways to approach the study of such a complex problem as head injury. Clinical evaluations, human volunteer studies, numerical models, and cadaver tests all provide important information in furthering the understanding of the tolerance of the human body to injury. Ultimately, though, the mechanism for injury lies within the cells that make up the whole organism. The way in which these cells respond to an external insult and the cascade of events triggered by this initial response combine to determine the severity of the injury. Information from the more macroscopic approaches provides a framework within which the mechanism of injury to the cell can be investigated.

Nonimpact acceleration of the head causes movement of the brain relative to the skull which results in deformation of the brain tissue. The extent of tissue deformation is a function of kinematic parameters of the head motion and of physical characteristics such as skull geometry and brain mass. Experimental work in which subhuman primates were subjected to inertial rotational head acceleration allowed the effect of several kinematic parameters on injury outcome to be investigated [6]. In particular, it was found that decelerations on the order of 10^5 rad/sec^2 over 6-10 msec directed along the coronal plane of the primate head resulted in a continuum of diffuse brain injuries ranging from mild concussion to diffuse axonal injury with coma.

The development of physical models of both primate and human skulls containing surrogate brain material provided a necessary link in relating the loading conditions of the whole head to the motion of the brain tissue itself. The deformation of the surrogate brain material within the model skull was tracked by filming a grid, imbedded in the gel, during model acceleration. An acceleration waveform from a representative physical model experiment is shown at the top of Figure 1 [3]. A reconstruction of a coronal plane grid in

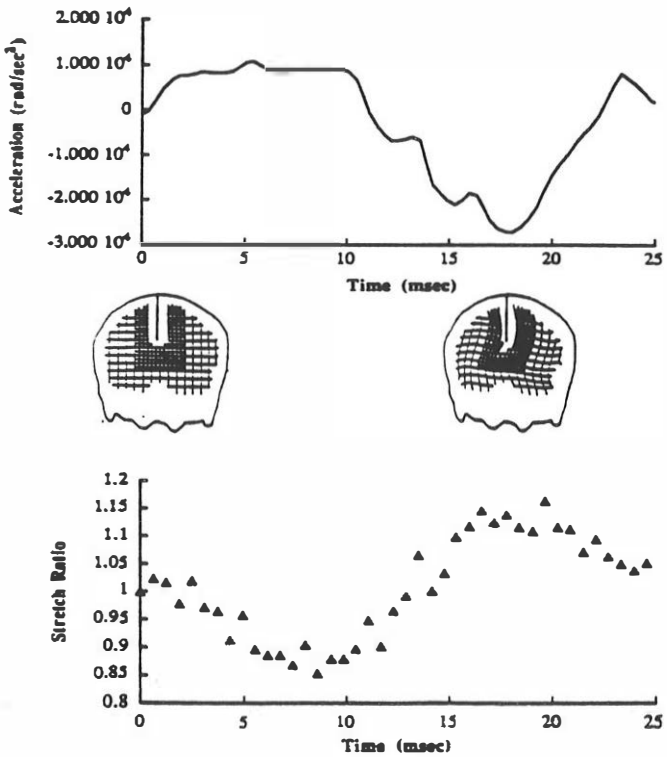

FIGURE 1

the model is shown at rest and at peak deceleration to illustrate the grid deformation seen. The shear strain of a particular grid element, in a location corresponding to that of the deep white matter of the brain, for example, can be calculated over the time course of the model acceleration. This calculated strain, plotted in the lower portion of Figure 1, provides an estimate of the strain that the deep white matter of the brain experiences during the inertial loading.

The effect of such strain on the pathophysiology of neural tissue can be investigated using isolated nerve preparations. The mechanical input of an isolated tissue can be more accurately described than in the whole brain, and the external environment of the tissue can be controlled. The goal then would be to describe the levels of dynamic strain that lead to functional and structural injury. Studies on the unmyelinated squid axon demonstrated graded levels of injury in response to rapid uniaxial elongation [7]. One of the several variables measured as indices of injury severity was the axon intracellular calcium concentration. Using a custom-made ion-selective calcium microelectrode inserted longitudinally into the 500-1000 micron diameter squid axon, the calcium concentration was found to increase following dynamic stretch of the axon. Figure 2 is a composite of these experiments; note that increasing the level of dynamic strain resulted in both an increase in peak $[Ca^{2+}]_i$ and a slower recovery to the initial level of calcium. Above a stretch ratio of 1.15, calcium remained elevated, suggesting a sustained functional deficit. For an elongation greater than 20%, the $[Ca^{2+}]_i$ continued to increase toward the level of calcium in the external bath, indicating axon function was completely compromised. Furthermore, it was found that dynamic stretch above 25% resulted in structural failure of the squid axon.

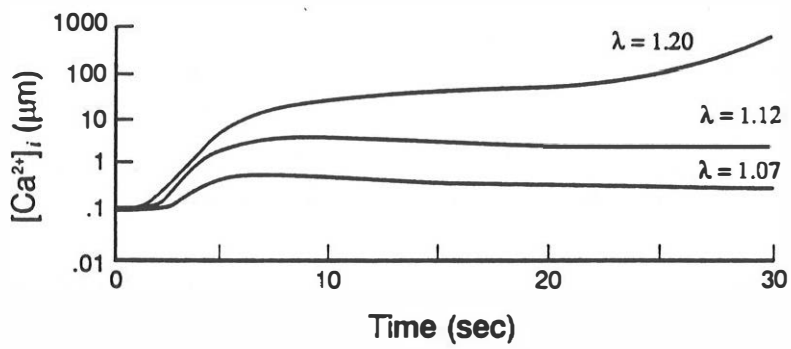

FIGURE 2

The unmyelinated squid axon is a well studied and convenient isolated axon preparation. However, in addressing the development of an injury tolerance level for myelinated axons in the brain as well as the mechanism of this injury at the cellular level, the differences between squid axons and myelinated nerves become important. The squid axon is structurally uniform along its length, whereas myelinated nerve fibers are punctuated at regular intervals by nodes of Ranvier. The nodes represent not only structural discontinuities, but also unique regions along the fiber for ion transport, considering the absence of the myelin barrier and the nonhomogeneous distribution of ion channels between the node and internode. For these reasons, the response of a single myelinated nerve fiber preparation to rapid dynamic strain is currently being studied. Presented here are data on the effect of uniaxial stretch on the intracellular free calcium concentration of myelinated nerves.

METHODS

An isolated myelinated nerve fiber was placed in a small scale materials testing apparatus constructed on the stage of a Nikon inverted microscope. The system was designed to deliver a controlled dynamic uniaxial displacement pulse to the nerve and record several physical and biochemical variables over time.

A single nerve fiber was isolated from a branch of the sciatic nerve bundle innervating the gastrocnemius muscle of a frog (*Rana pipiens*). After locating this branch, the connective tissue sheath enclosing the individual fibers within the nerve branch was split open and cut away. The exposed nerve fibers were then gently spread apart. A single fiber was selected for study and all other nerve fibers were cut away, isolating 6 -10 mm of the single myelinated nerve. Myelinated fibers were, on average, 12-15 microns in diameter.

The single fiber, still attached at one end to the sciatic nerve bundle and at the other to the gastrocnemius muscle, was transferred onto a 0.17 mm glass cover slide on the microscope stage. The nerve, bathed in room temperature Ringer's solution, was then mounted into custom-made glass micropipets. The pipets were constructed in a two step process from 1.19 mm glass capillary tubing (Drummond Scientific). First, the tubing was drawn to a 15-20 micron inner diameter tip on a pipet puller. Second, an internal taper was fashioned several hundred microns from the tip by applying heat locally to the pipet as it hung vertically in a microforge. This taper reduced the inner diameter to 5-10 microns.

The movement of each pipet, positioned horizontally on the microscope stage, was controlled by micromanipulators (Narishige, model ML-8). To mount the myelinated nerve in the micropipets, one pipet was positioned close to an end of the isolated length of single fiber and a vacuum was applied through the pipet to pull the fiber into the pipet tip. The sciatic nerve bundle and the muscle were then cut away, and the free end of the single fiber was drawn into the second pipet, again using a vacuum. The taper inside the micropipet tip prevented the fiber from moving into the pipet shaft. To promote bonding of the myelinated fiber to the inner wall of the glass pipets, the pipets were silanized and coated with 1% glutaraldehyde (Aldrich Chemical) prior to the mounting procedure. An isolated myelinated fiber held in micropipets is shown schematically in Figure 3.

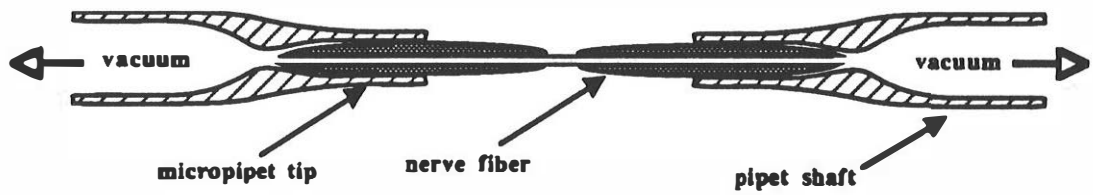

FIGURE 3

During dynamic elongation of the nerve, one pipet remained stationary. As depicted in Figure 4, the other pipet was linked by a pulley to an electromagnetic actuator. The magnitude and risetime of the actuator input pulse were controlled using a sweep generator (Krohn Hite, model 1600) which was triggered by computer to send a single pulse to the actuator. The resultant displacement pulse was measured by an angular displacement transducer (Trans-Tek, model 0604-000) attached to the pulley on the microscope stage. Software written for a Dell 310 computer equipped with a MetraByte Model DAS-16F high speed A/D expansion board allowed acquisition of four channels of data before and after triggering the stretch.

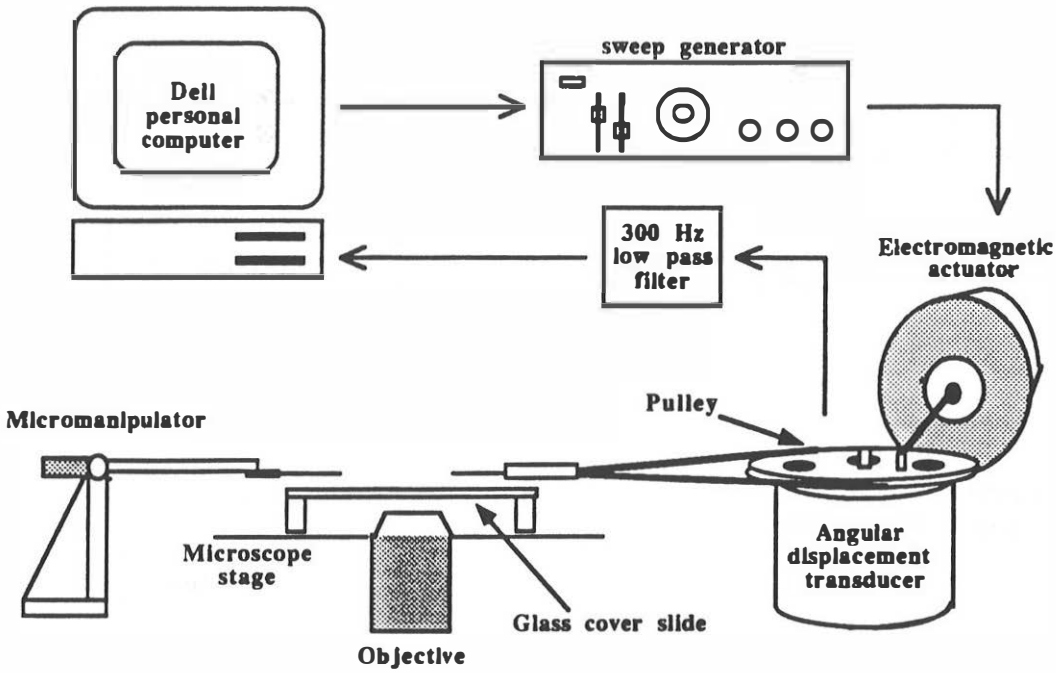

FIGURE 4

Fluorescence Measurements

The intracellular free calcium concentration of the single nerve fiber was monitored following dynamic elongation as a means of assessing the severity of an injury below the structural failure limit of the nerve. Calcium measurements were made using the fluorescent calcium indicator dye, fura-2 (Molecular Probes). The fluorescence characteristics of the dye molecule are altered when the dye binds to calcium, thus the intensity of the fluorescence from unbound and bound dye can be used to determine intracellular free calcium concentrations.

To load the nerve with dye before mounting it in micropipets, the single fiber was incubated at room temperature for 45-60 minutes in a solution of fura-2 acetoxymethyl ester. This lipid soluble form of the dye diffuses into the nerve where endogenous esterases cleave the acetoxymethyl ester creating a lipid insoluble dye molecule that binds to ionic calcium. Upon binding calcium, the excitation spectrum for the fluorescent dye shifts. The unbound dye fluoresces maximally when excited with approximately 360 nm wavelength light, whereas the peak for calcium-bound fura-2 is near 340 nm. Therefore, a ratio of the intensities of the fluorescence emitted from the nerve at two distinct excitation wavelengths can be used to calculate the intracellular free calcium concentration. This calculation and the supporting theory are described in detail elsewhere [2].

The system used to excite the nerve fiber and measure the emitted fluorescence is shown in Figure 5. Ultraviolet light generated by a Xenon lamp passed through a rapidly rotating filter wheel (Johnson Foundation, University of Pennsylvania) containing 340 nm and 380 nm filters. The fiber was excited once, then, by each of the two wavelengths for every rotation of the filter wheel. The fluorescence emitted from the nerve passed through a 510 nm filter and into a photomultiplier tube (Hamamatsu Corp., model R928). The output from the photomultiplier tube was amplified, filtered, and separated into two signals, one

corresponding to 340 nm excitation, the other to 380 nm. Two channels controlled by the system software were used to acquire these signals before and after the dynamic elongation of the nerve. The ratio of the two signals was computed after subtracting the background fluorescence. The $[Ca^{2+}]_i$ was then calculated from this ratio using a linear fit to the calibration curve obtained for the system by testing a series of calcium standards.

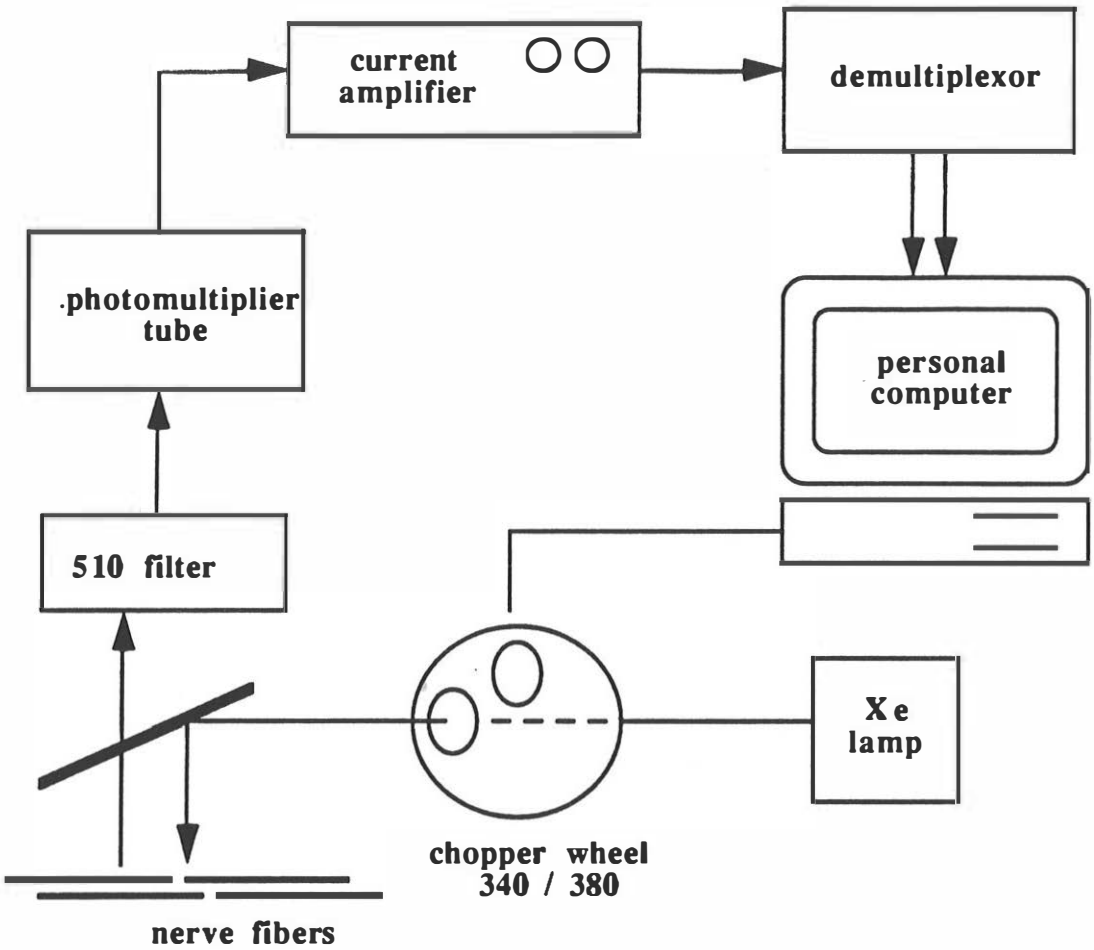

FIGURE 5

RESULTS

The time course of the change in intracellular free calcium, $[Ca^{2+}]_i$, in myelinated nerve fibers treated with a calcium ionophore is shown in Figure 6. A calcium ionophore effectively increases the cell membrane permeability to divalent cations, with a high degree of selectivity for calcium. The intracellular free calcium concentration of the nerve fibers loaded with fura-2 dye was initially about 200 nM. After 15-20 seconds the ionophore 4-bromo A23187 (Molecular Probes) was added to the Ringer's solution bathing the nerves. The level of calcium in the nerves then rose, surpassing 600 nM in two minutes. Typically, the concentration continued to increase toward the 1 mM level of calcium in the external bath. Note that in Figures 6-8, polynomial curve fits to the data are plotted superimposed on the individual data points to illustrate general trends.

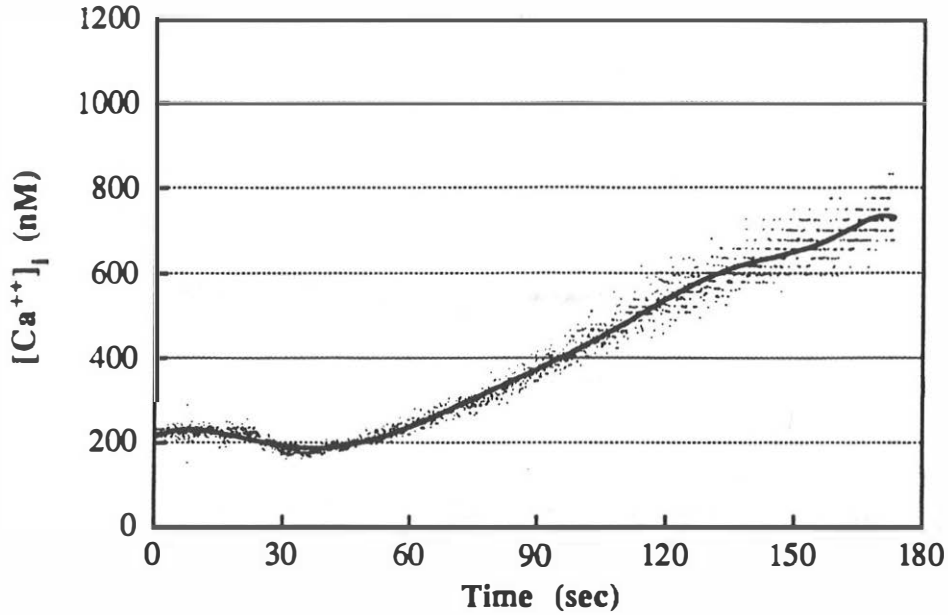

FIGURE 6

The effect of a dynamic elongation on the intracellular calcium concentration of myelinated nerves was first studied in a preparation of 8-12 nerve fibers. These nerves, attached at each end to the nerve bundle, were held in glass capillary tubing rather than micropipets. The length of the fibers, taken as the distance between the ends of the tubing,was 8-10 mm. The initial, or resting level, of calcium in the myelinated nerves was just above 100 nM as shown by the first segment in Figure 7 (on average, several minutes separate each segment of data). The fibers were subjected to a rapid uniaxial displacement pulse of 2 mm, as described above. Immediately following the stretch, the intracellular free calcium concentration rose, reaching approximately 160 nM in 60 seconds and then plateauing. Several minutes later, the calicum concentration had decreased slightly, as evidenced by the third segment of Figure 7. A second, larger, displacement pulse of about 3 mm was then applied to the nerve fibers; this again resulted in an increase in the intracellular calcium.

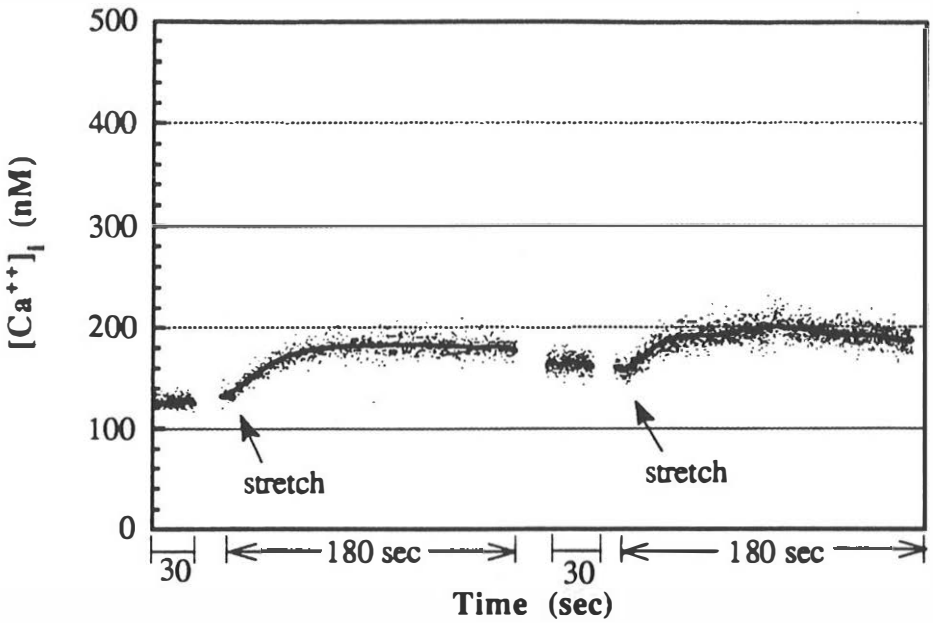

FIGURE 7

A similar series of experiments was performed on a single isolated myelinated fiber, loaded with fura-2 dye and mounted in glass micropipets. The length of the nerve fiber isolated between the pipet tips was 6-7 mm. The calcium concentration prior to the mechanical insult was measured twice and found to be near 100 nM, as shown by the first two segments of the calcium data in Figure 8a. After rapidly stretching the single fiber approximately 1-1.5 mm, the $[Ca^{2+}]_i$ increased slightly over 30 seconds to exceed 200 nM, and then gradually declined. The last segment of Figure 8a represents the concentration several minutes after this first stretch. These data are also plotted for reference in Figure 8b to show the $[Ca^{2+}]_i$ in the single nerve preceding a second applied displacement pulse. This second stretch of 1.5-2 mm elicited an increase in the intracellular free calcium concentration which continued over the two minutes shown, reaching nearly 1 μM.

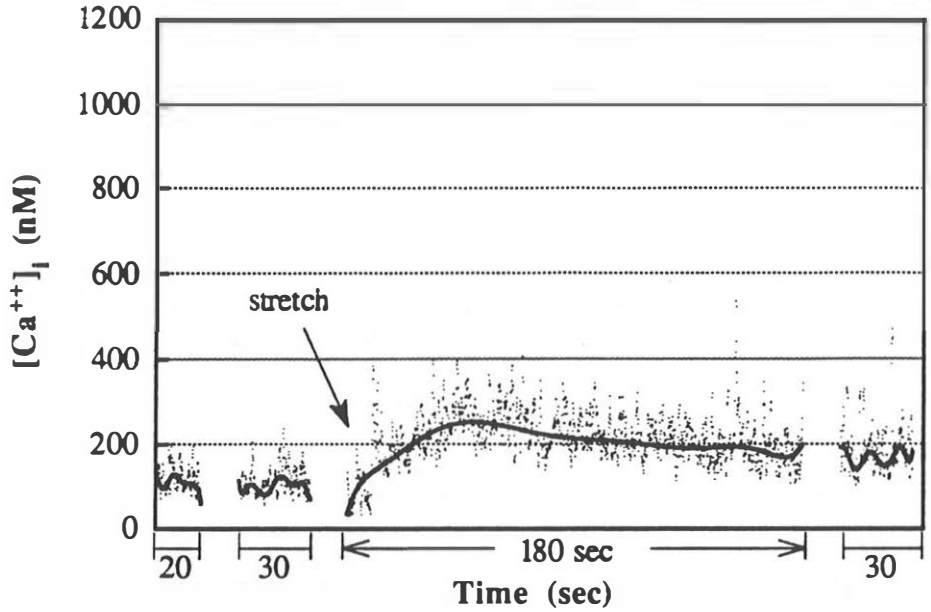

FIGURE 8A

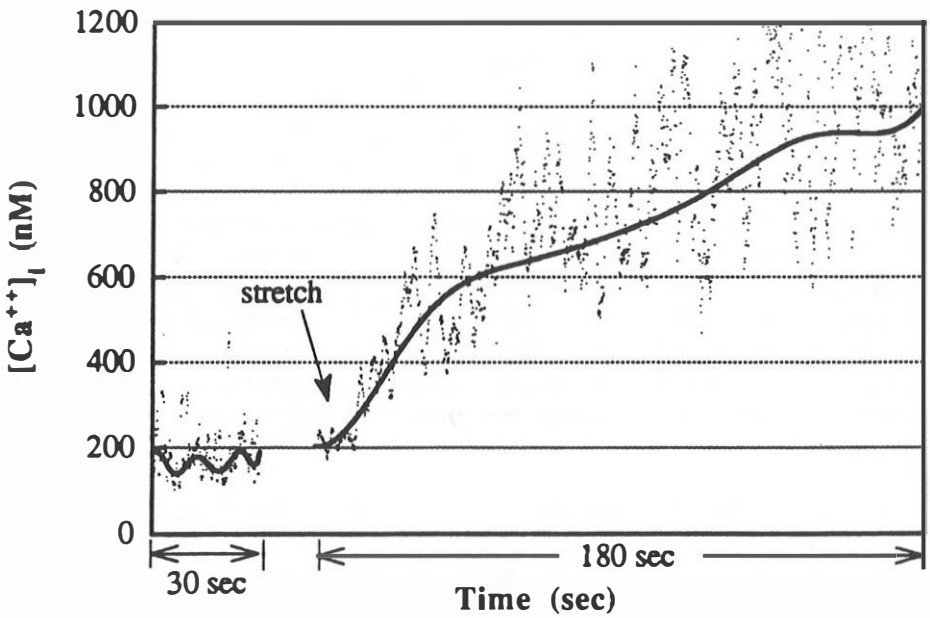

FIGURE 8B

DISCUSSION

The small diameter of myelinated nerves prohibits the use of intracellular calcium microelectrodes such as those used previously in the squid axon. Advancing our study of dynamic stretch injury from unmyelinated axons to myelinated nerves required finding a suitable technique for measuring intracellular calcium. The results of the experiments just described indicate that the fluorescent dye fura-2 can be used to measure the intracellular free calcium concentration noninvasively in a single myelinated nerve fiber preparation.

By treating the nerve with a calcium ionophore an increased $[Ca^{2+}]_i$ was demonstrated in response to a chemically induced increase in membrane permeability. Increased intracellular calcium was also seen immediately following dynamic elongation of myelinated nerves. The response of a single fiber was similar to that of a group of fibers; both exhibited a similar time course for the calcium transient and the ability to respond to a second stretch. Thus, myelinated nerve fibers show stretch sensitivity as indicated by intracellular calcium, much like that demonstrated in the unmyelinated axon.

We hypothesize that stretch induced intracellular calcium transients result directly from the mechano-poration of the cell membrane. That is, by imposing a dynamic strain on the axolemma, transient defects are created which lead to an increased membrane permeability. These nonspecific transient membrane openings would allow calcium to diffuse into the axon from the extracellular medium along its large concentration gradient. Elevated levels of ionic calcium are known to have detrimental effects on both the function of a nerve cell and its internal structure [1, 4]. The extent of damage, or injury, done by the calcium would depend on the balance between the amount and rate of calcium entering through the impaired membrane and the ability of the nerve to rid itself of this excess calcium. Differing outcomes, then, would be expected from increasing dynamic strains, covering the spectrum from mild, reversible injury to cell death.

This is precisely the transfer function we would like to develop for myelinated nerves, i.e. the relationship between dynamic strain and the extent of injury to the fiber, expressed here through intracellular calcium measurements. It should be pointed out that a stretch ratio based on the entire fiber length may not be the most appropriate way to characterize the strain. Because the myelinated fiber is structurely nonhomogeneous, the strain experienced at the node of Ranvier, the paranodal region, and the internode could be significantly different. Schneider measured the elongation of several segments along a single fiber during quasi-static stretch and found the greatest strain in the internode [5]. The different regions along the fiber are therefore likely to have varying degrees of vulnerability to stretch. This emphasizes the importance of extending the development of isolated tissue tolerance criteria from unmyelinated axons to the more complex myelinated nerves. In future work, the spatial distribution of intracellular calcium changes will be investigated in order to better understand the influence of the structural nonhomgeneity of myelinated nerves.

The experimental system described in this paper will provide the data to quantify strain dependent changes in the intracellular free calcium concentration in myelinated nerves, which in turn will lead to the development of a functional failure criterion. Such a criterion is important in the interpretation of experimental and numerical simulations attempting to describe tissue deformation occurring from impact or impulsive loads.

ACKNOWLEDGEMENTS

The authors would like to thank Drs. K. Beyenbach and D. Zimmer for the use of equipment at Cornell University during micropipet construction. This research was supported by a grant from the Centers for Disease Control.

REFERENCES

1. Chan, S.Y., S. Ochs, and R.A. Jersild Jr., *Localization of Calcium in Nerve Fibers.* J. Neurobiol., 1984. **15**(2): p. 89-108.

2. Grynkiewicz, G., M. Poenie, and R.Y. Tsien, *A New Generation of Ca^{2+} Indicators with Greatly Improved Fluorescence Properties.* J. Biol. Chem., 1985. **260(6)**(March 25): p. 3440-3450.

3. Margulies, S.S., L.E. Thibault, and T.A. Gennarelli, *Physical Model Simulations of Brain Injury in the Primate.* J. Biomechanics, 1990. **23**(8): p. 823-836.

4. Schliwa, M., *et al.*, *Calcium Lability of Cytoplasmic Microtubules and its Modulation by Microtubule-Associated Proteins.* Cell Biol., 1981. **78**(2): p. 1037-1041.

5. Schneider, D., *Die Dehnbarkeit der Markhaltigen Nervenfaser des Frosches in Abhängigkeit von Funktion und Struktur.* Z. Naturforschg., 1952. **7b**: p. 38-48.

6. Thibault, L.E. and T.A. Gennarelli, *Brain Injury: An Analysis of Neural and Neurovascular Trauma in the Non-human Primate.* AAAM, 1990. **34**: p. 337-352.

7. Thibault, L.E., *et al.*, *The Strain Dependent Pathophysiological Consequences of Inertial Loading on Central Nervous System Tissue.* Proceedings of IRCOBI, 1990. **19**: p. 191-202.